Proceedings of the 4th International Conference on Fluid Flow and Thermal Science (ICFFTS'23)
Lisbon, Portugal- December 07 - 09, 2023
Paper No. 168
DOI: 10.11159/icffts23.168

Performance of a Metal Foam Coated Airfoil Tube Cross-Flow Heat Exchanger

Raghad Ahmed Ali Alsereidi, Guan Qiangshun, Khloud Alseiari, Fatima Alzeyoudi, MD Didarul Islam, Afshin Goharzadeh, Yap Yit Fatt*
Department of Mechanical Engineering, Khalifa University of Science and Technology,
P.O. Box 127788, Abu Dhabi, United Arab Emirates
100045461@ku.ac.ae; qiangshun.guan@ku.ac.ae; 100049692@ku.ac.ae,
100049787@ku.ac.ae; didarul.islam@ku.ac.ae; afshin.goharzadeh@ku.ac.ae; *yap.fatt@ku.ac.ae

Abstract **-** This study presents a numerical study of the heat transfer and pressure drop characteristics of airfoil tube with porous metal foam in crossflow. A unified modelling approach is used to model the flow and heat transfer in the simulation domain. The model is first verified and validated against circular tube forced convection problem with known empirical relation. Then, the effects of airfoil shape parameters and metal foam properties are studied. Among these, airfoil thickness is the most significant parameter, and the performance index increases as foam thickness and permeability increase, while it decreases with the increase of porosity.

Keywords**:** Heat exchanger; Cross-flow; Airfoil tube; Metal foam; Porous media model; Equilibrium thermal model

1. Introduction

Crossflow tube bundle heat exchangers are extensively used in a wide range of industrial systems such as evaporators, condensers, super-heaters, economizers, etc. [1]. Circular tube shape is a commonly used geometry owing to its large surface area per unit length and the ease to fabricate using standard manufacturing processes. However, circular tube is a bluff body to the external flow and therefore normally induces a high pressure drop. To achieve better performance, tube with a larger heat transfer area and more streamlined tube have been designed including elliptical [2], oval [3], cam-shaped [4], and airfoil [5] tubes. Apart from tube cross section, surface modification techniques have also been developed for further heat transfer augmentation, e.g., finned [6], dimpled [7], and metal foam surfaces [8]. The primary benefit of introducing a metal foam stems from its favourable high thermal conductivity and high permeability for compact heat exchangers. The integration of fins and metal foam has been demonstrated to improve the heat transfer efficiency of PCM heat storage unit [9]. However, to the best of our knowledge, the combination of airfoil tube with porous metal foam has not been explored so far. Herein, this work aims to numerically study the synergy of airfoil shape and metal foam on the thermo-hydraulic performance in crossflow. A systematic parametric study is performed to reveal the effects of shape parameters and foam properties.

2. Mathematical Formulation

Figure 1 shows a crossflow configuration of a non-circular tube constrained in a fluid channel, where a hot fluid flowing internally within the tube and a cold fluid flowing externally across the tube. To improve the thermo-hydraulic performance, a porous metal foam is coated around the tube in view of its high thermal conductivity and high permeability. In such a basic operation unit, heat is transferred from the internal hot fluid to the tube internal surface convectively, through the tube wall and metal foam conductively, and then from the metal foam external surface to the external cold fluid convectively. The above heat transfer is in the reversed direction for the configuration of a cold internal fluid and a hot external fluid. The two regions in the channel, i.e., the fluid Ω_f and the porous metal foam Ω_m , are separated by the fluid-foam interface Γ. We note that within the unified modelling approach that we adopted, there is no need to match the boundary conditions at Γ. All the other boundary conditions as well as the initial condition are specified respectively as follows:

- At the channel inlet, boundary conditions with constant velocity (u_{in} , $v_{in} = 0$) and temperature T_{in} are specified.
- No slip condition (i.e., $u = v = 0$) is imposed at all the walls.
- The channel wall is thermally insulated ($\partial T/\partial y = 0$), while tube external wall is fixed at temperature T_{hot}.

- At the outlet, outflow boundary condition is enforced with heat carried only by convection ($\partial T/\partial x = 0$).
- Fluid at temperature T_{in} is assumed initially quiescent in the channel.

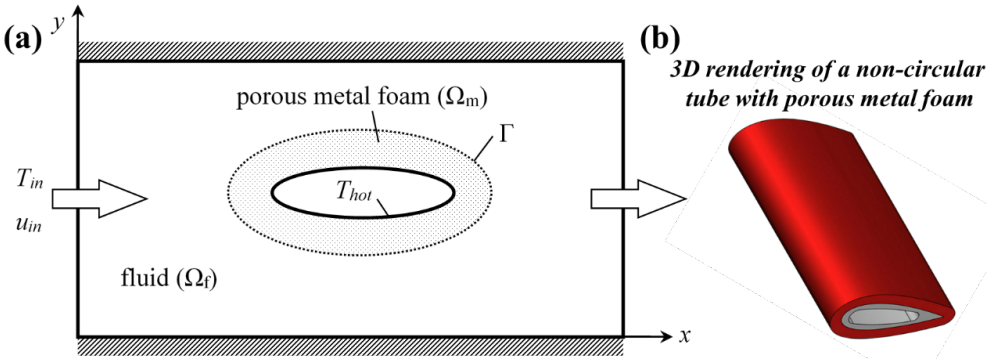

Fig. 1: Schematic of a crossflow single non-circular tube wrapped with a porous metal foam in a fluid channel.

Herein, we use a unified approach [10] to model the flow and heat transfer in the combined domain $\Omega_f \cup \Omega_m$ by assuming that the fluid and metal foam reach thermal equilibrium locally (i.e., $T_f = T_m = T$), with no net heat transfer from one region to the other. In this case, the conservation equations governing the transport of mass, momentum and energy in the entire domain $\Omega_f \cup \Omega_m$ are given by

$$\nabla \bullet \vec{u} = 0 \tag{1}$$

$$\frac{\partial(\rho_f \vec{u})}{\partial t} + \nabla \bullet (\rho_f \vec{u}\vec{u}) = -\nabla p + \nabla \bullet \left[\mu_f (\nabla \vec{u} + \nabla \vec{u}^T)\right] + S_{\vec{u}} \tag{2}$$

$$\frac{\partial[(\rho c)_{ave} T]}{\partial t} + \nabla \bullet \left[(\rho c)_f \vec{u} T\right] = \nabla \bullet (k_{ave} \nabla T) \tag{3}$$

where $\vec{u}$, p and T are respectively velocity, pressure and temperature. The thermo-physical properties are density ρ, viscosity μ, specific heat c and thermal conductivity k. The subscripts f, m and ave represent quantities associated respectively to the fluid, metal foam and average. These properties are determined as

$$(\rho c)_{ave} = \begin{cases} (\rho c)_f, & \vec{x} \in \Omega_f \\ (1-\varepsilon)(\rho c)_m + \varepsilon(\rho c)_f, & \vec{x} \in \Omega_m \end{cases} \tag{4}$$

$$k_{ave} = \begin{cases} k_f, & \vec{x} \in \Omega_f \\ (1-\varepsilon)k_m + \varepsilon k_f, & \vec{x} \in \Omega_m \end{cases} \tag{5}$$

The third term on the right-hand side of Eq. (2), $S_{\vec{u}}$, forces the flow in the metal foam of porosity ε and permeability K into the Carman-Kozenay flow in porous media [11], which is given by

$$S_{\vec{u}} = \begin{cases} 0, & \vec{x} \in \Omega_f \\ -A\dfrac{(1-\varepsilon)^2}{\varepsilon^3 + B}\vec{u}, & \vec{x} \in \Omega_m \end{cases} \tag{6}$$

where $A = 10^9$ and $B = 0.005$ [12].

For numerical solution of the above equations, the physical domain is discretized into non-overlapping finite control volumes. Solution of the governing conservation equations is performed using ANSYS Fluent 2022R1 with a pressure-based based solver. The velocity-pressure coupling is handled using the default coupled scheme with second-order spatial discretization. The maximum number of iterations is set to 5000. The steady-state simulation is deemed to be convergent when the residuals of all relative variables are less than 10^{-6}.

3. Results and Discussion

3.1. Effects of Porous Metal Foam

For verification and validation purposes, we take a circular tube as an example to simulate the flow and heat transfer characteristics. Given with $T_{in} = 293$ K, $u_{in} = 4.019\times10^{-4}$ m/s, $T_{hot} = 353$ K, $H = L = 0.6$ m, $D = 0.1$ m, and $\delta = 0.02$ m, the average Nusselt number for forced convection over a circular cylinder in crossflow can be evaluated using the empirical relation: $Nu_{avg} = 0.911Re^{0.385}Pr^{1/3}$ [13] Taking water as the working fluid and evaluating all properties at $T_{avg} = (T_{in} + T_{hot}) / 2 = 323$ K, we have $Re = 40$, $Pr = 6.99$, and hence the theoretical $Nu_{avg} = 7.21$. From our mesh-independent simulation results, the average surface heat transfer coefficient at the internal tube wall is $h = 43.66$ W/m^{2}K, which yields the predicted $Nu_{avg} = hD/k = 7.28$. The closely matched results show the validity of our simulation.

Then, we investigate the effect of adding a porous metal foam over both circular and airfoil-shaped tubes. We observe that with the addition of metal foam the heat transfer rate considerably enhanced from $h = 43.66$ to 51.06 W/m^{2}K for circular tube, and the enhancement got amplified from $h = 483.22$ to 735.57 W/m^{2}K for an airfoil tube at a larger $u_{in} = 2.01\times10^{-3}$ m/s. In addition, Nu_{avg} was improved from 7.28 to 8.51 and from 16.11 to 24.52 for circular and airfoil tubes respectively. To understand the mechanism of enhanced heat transfer, we plotted the steady-state u, p and T fields in Figs. 2 and 3.

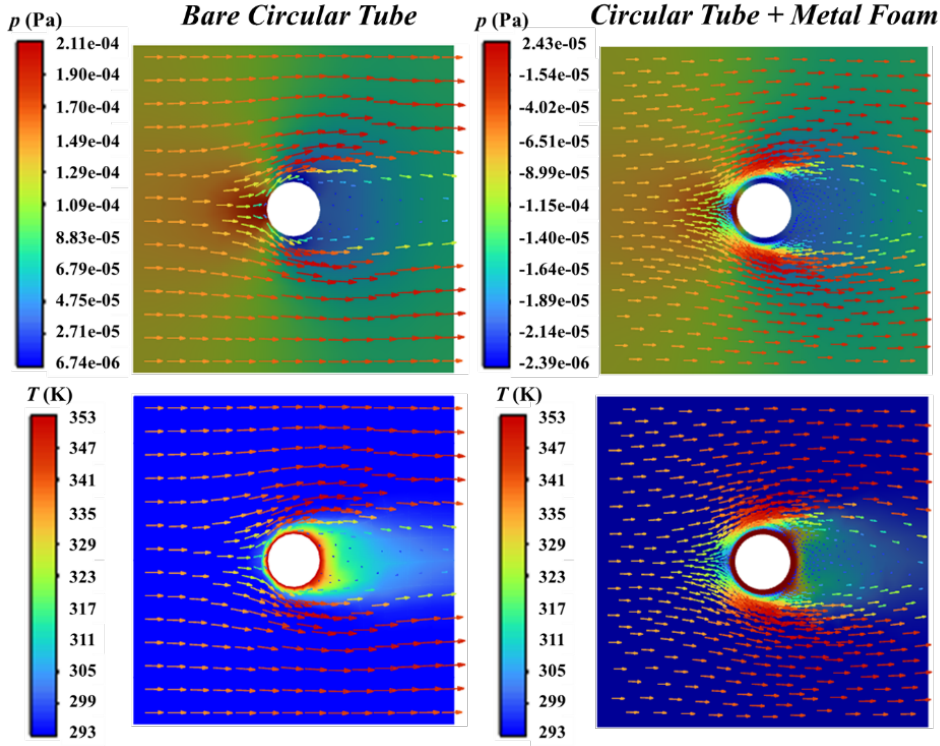

Fig. 2: Velocity, pressure and temperature fields for bare circular tube (left) and circular tube with metal foam (right).

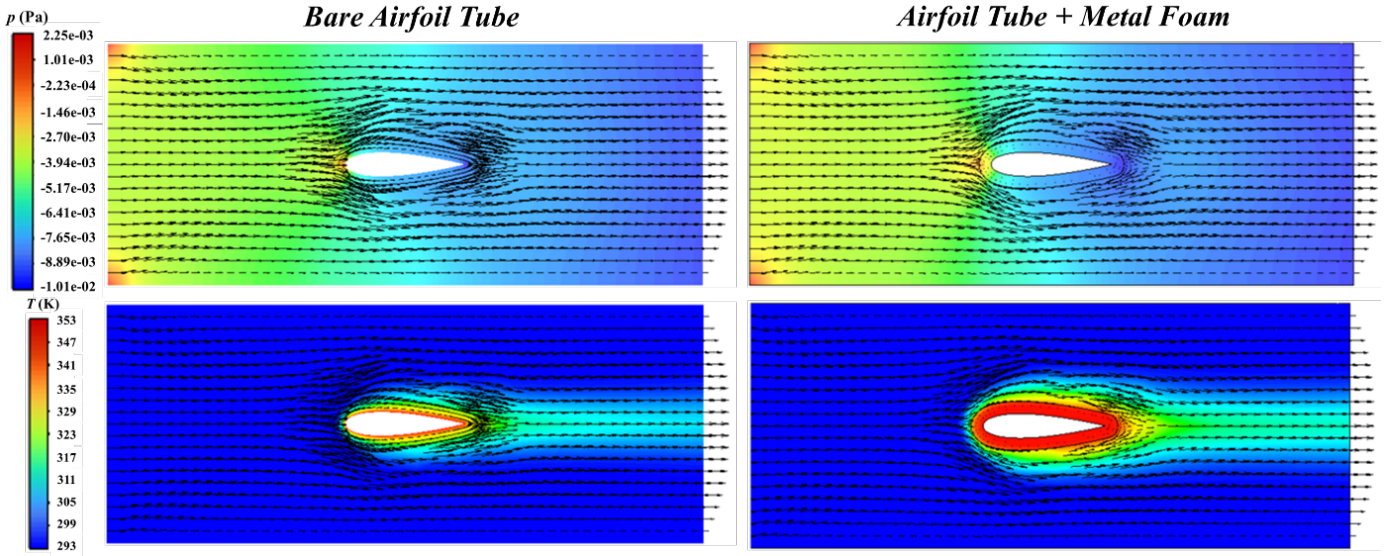

Fig. 3: Velocity, pressure and temperature fields for bare airfoil tube (left) and airfoil tube with metal foam (right).

When the fluid flows from the inlet to the outlet, the flow is obstructed by the presence of internal tube causing large pressure difference between upstream and downstream (top panel of Fig. 2). In the resultant wake region, the fluid flow is comparatively slow, which significantly reduces the level of convective heat transfer (bottom of Fig. 2). Using an airfoil-shaped tube, the undesired wake region was effectively suppressed as demonstrated by the more streamlined fluid flow in Fig. 3. With the addition of porous foam layer, the heat transfer rate can be further improved considering its high thermal conductivity. However, in the meanwhile, the pressure drop was increased from 5.59×10^{-5} to 6.30×10^{-5} Pa and from 7.70×10^{-3} to 1.01×10^{-2} Pa for the circular and airfoil tubes respectively. This blockage effect was observed even at a low Reynold number, where the boundary layer is fully developed and laminar. Compared to a solid metallic coating, metal foam is therefore favoured for minimizing the increase in pressure drop in view of its high porosity and permeability. As seen from the bottom panel of Fig. 3, the combination of airfoil shape and metal foam results in obvious heat transfer enhancement.

3.2. Effects of Airfoil Tube Geometry

To obtain an enhanced heat transfer mechanism for a better heat exchanger design, the effects of airfoil geometrical parameters (i.e., maximum camber M, maximum camber position P, maximum airfoil thickness XX, and angle of attack θ) on the cross-flow heat exchanger performance were systematically investigated, where the flow features, local heat transfer coefficient, Nusselt number, and pressure drop are examined in detail. We use the traditional NACA 4-digit specification (i.e., NACA-$MPXX$) and the chord length to define the shape of airfoil tube. The standard case is: NACA-0030, chord length of 10 mm, angle of attack of 0°, aluminium metal foam with porosity of 0.85 and thickness of 1 mm.

Four different NACA airfoil cross sections (0330, 3330, 6330, and 9330) are compared for the purpose of studying the effect of the first digit M, which represents the length percentage of maximum camber line relative to chord length. With the increase in M, the airfoils become asymmetrical as the curvature of the camber line gets larger. The average Nusselt number (Nu), pressure drop (Δp) and performance index (PI) are compared in Fig. 4. The NACA-3330 airfoil tube obviously achieved the highest overall efficiency by maximizing Nu and minimizing Δp. With further increase in M, Nu slightly decreases when Δp increases, and therefore PI gets smaller. This result claims that small curvature in the leading edge can effectively enhance the overall efficiency of the heat exchanger when fixing all the other parameters.

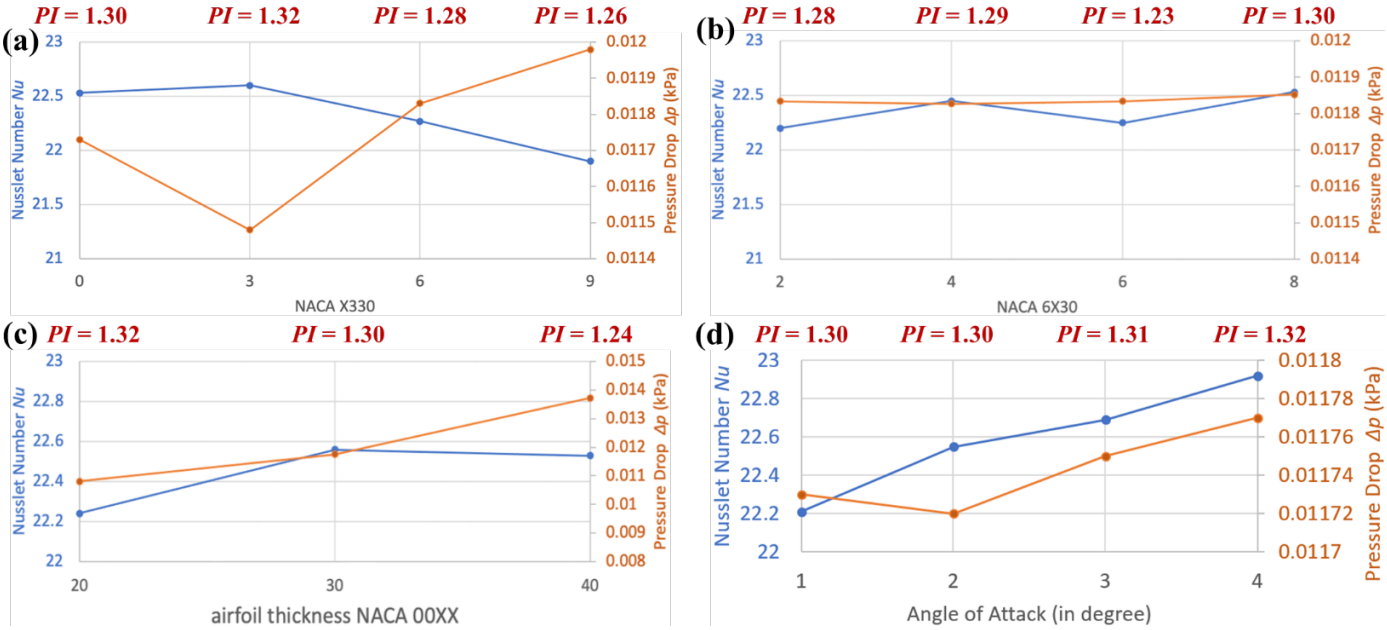

Fig. 4: Effects of NACA *MPXX* 4-digits (a) *M*, (b) *P*, (c) *XX*, and (d) angle of attack.

The second digit *P* of NACA airfoil characterizes the location of maximum camber relative to the chord length. Four different cases have been studied (i.e., 6230, 6430, 6630,6830). According to Figure 4, *Nu* shows inconsistent changes while increasing *P*. NACA-6830 airfoil tube undergoes higher mixing after the trailing edge compared to NACA-6630. As a result, NACA-6630 has a value of *Nu* = 22.44 which is lower than that of NACA-6830 (22.53). As for Δp, it is not remarkably influenced by the second digit compared to what we witnessed on the first digit as the shape does not change much when changing the second digit *P*. Among the four cases, NACA-6830 achieves the highest *Nu*. However, the increase of *Nu* with the expense of Δp cannot be neglected as NACA 6830 also has the highest pressure drop.

The last two digits *XX* was increased from 20 to 40 for symmetric airfoil tubes. NACA-0020 airfoil has a maximum thickness of 20% of its chord length. This means that the distance between the upper and lower surfaces of the airfoil is 20% of the chord length at its thickest point. Airfoil thickness plays a role in improving the crossflow heat exchanger compactness. Increasing *XX* from 20 to 30 contributed to enhancing the heat transfer at the leading edge because the increase of the frontal areas leads to a jet flow effect [14]. However, a slight fall was observed with further increase to 40 as large thickness causes high-intensity reverse flow at the trailing edge.

Angle of attack θ refers to the angle between the chord line and the relative stream. In practical applications, exposing the flow on a heat exchanger tube might cause a slight deviation from the symmetric axis of the cross section. Therefore, we varied the angle of attack in a small range for $0° \leq \theta \leq 4°$. It was discovered that both *Nu* and Δp increase as θ increases, while *PI* also increases, indicating better heat transfer effectiveness. Further increase in θ will cause flow separation. For the tube arrangements from $5° \leq \theta \leq 15°$, fluid flow is greatly affected by channel blockage, and hence *PI* reduces.

3.3. Effects of Metal Foam Properties

Since the flowing fluid will pass through the pores of metal foam, the foam properties inherently affect the heat transfer and pressure drop characteristics. Herein, we have studied the effects of foam material, metal foam thickness, foam porosity and permeability.

Three metal foam materials were examined, namely, aluminium (Al), copper (Cu), and stainless-steel (SS), which are the most commonly used materials for manufacturing heat exchanger and internal tubes. Both Al and Cu are known for their high thermal conductivity, and SS is widely used for tubes at high-temperature conditions in view of its strength, durability,

and especially high resistance to corrosion. Among the three materials, Cu has the highest thermal conductivity, which means that it normally transfers heat quickly and efficiently. However, this may also affect the temperature distribution and flow patterns around the airfoil tube. To link heat transfer to both properties, thermal diffusivity is used to measure how effective the heat transfer process is. Therefore, as shown in Fig. 5, Cu achieves the highest heat transfer rate due to its highest thermal diffusivity among the three materials.

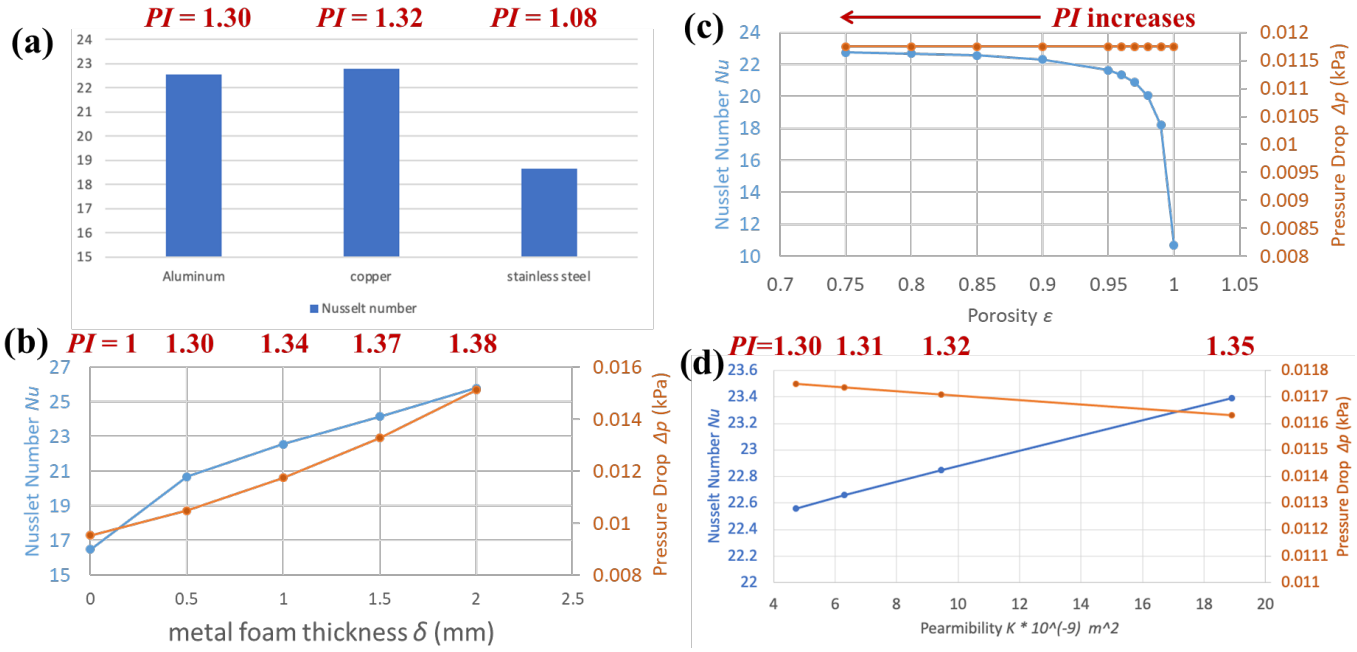

Fig. 5: Effects of (a) metal foam material, (b) foam thickness, (c) porosity, and (d) permeability.

Then, we studied the effect of metal foam thickness on Δp and Nu with 5 different thicknesses (0, 0.5, 1, 1.5, and 2 mm). Figure 5 shows that metal foam thickness has a significant effect on Δp. A thicker metal foam will generally have a higher Δp because as foam thickness increases, the number of pores also increases through which the fluid has to penetrate, causing a higher flow resistance. However, the relationship between foam thickness and Δp is not linear since no matter how thick the foam is, it will eventually become saturated and unable to accept additional fluid flow. In terms of the effect of metal foam thickness on Nu, it is generally observed that increasing foam thickness leads to an increase in Nu as the surface area available for heat transfer is increased accordingly.

Porosity ε measures the void space within its core, which is expressed as the ratio of all pores to the total volume. It is notable from Fig. 5 that Nu increases with a reduction in ε since porous media generally increase heat conduction. In addition, the effective thermal conductivity increases as ε decreases, which plays a vital role in reinforcing heat transfer. Moreover, the decrease in ε reduces permeability, which reduces natural convection, and thus weakening overall heat transfer. In contrast, Δp remains constant as porosity increases due to the fact that permeability does not change.

Permeability K characterizes how well the pores of metal foam are connected. In other words, a high K means that the pores allow the fluid to easily flow through the metal foam, leading to more effective heat transfer. This is manifested in Fig. 5 that as K decreased from 1.89×10^{-8} to 4.74×10^{-9} Nu decreased from 23.39 to 22.56 accordingly. However, it was observed that K and Δp follow an inverse relationship, which can be described by the Hazen-Darcy equation [15].

4. Conclusion

The heat transfer and pressure drop characteristics of airfoil tube coated with a porous metal foam layer are studied in this work using an unified CFD modelling approach. The model is first verified and validated for circular tube without

foam. Then, the effect of adding a porous metal foam on the thermo-hydraulic performance is investigated, which tends to increase heat transfer rate at the cost of higher pressure drop. A systematic parametric study has been performed to study the effects of airfoil geometrical parameters (i.e., NCAA 4 digits, and angle of attack) and metal foam properties (foam material, foam thickness, foam porosity and permeability). In all these cases studied, the overall performance index varies between 1.23−1.32. Among all the 4 digits, the maximum airfoil thickness *XX* is the most significant parameter that affects heat exchanger performance. Copper foam achieves a better performance in comparison to aluminium and stainless steel foams. The performance index increases as foam thickness and permeability increase, while decreasing with the increase of porosity.

References

[1] Q. Guan, H. Li, A. Goharzadeh, M.D. Islam, C.W. Kang, & Y.F. Yap, "Laminar cross-flow convective heat transfer of a finned cylindrical tube in the presence of particle deposition and deposit erosion", *Appl. Therm. Eng.*, 2023, pp. 121570.

[2] T.A. Ibrahim, & A. Gomaa, "Thermal performance criteria of elliptic tube bundle in crossflow", *Int. J. Therm. Sci.*, 2009, vol. 48, pp. 2148-2158.

[3] S. Tiwari, D. Maurya, G. Biswas, & V. Eswaran, "Heat transfer enhancement in cross-flow heat exchangers using oval tubes and multiple delta winglets", *Int. J. Heat Mass Transf.,* 2003, vol. 46, pp. 2841-2856.

[4] C.K. Mangrulkar, A.S. Dhoble, A.R. Deshmukh, & S.A. Mandavgane, "Numerical investigation of heat transfer and friction factor characteristics from in-line cam shaped tube bank in crossflow", *Appl. Therm. Eng.,* 2017, vol. 110, pp. 521-538.

[5] Y. Ito, N. Inokura, & T. Nagasaki, "Conjugate heat transfer in air-to-refrigerant airfoil heat exchangers", *J. Heat Transf.,* 2014, vol. 136, pp. 081703.

[6] E. Ibrahim, & M. Moawed, "Forced convection and entropy generation from elliptic tubes with longitudinal fins", *Energy Conv. Manag.*, 2009, vol. 50, pp. 1946-1954.

[7] H.V. Malapur, S.N. Havaldar, & G.A. Anderson, "Heat gain in an internally dimpled tube heat exchanger - A numerical investigation", *Mater. Today: Proc.*, 2023, vol. 72, 1530-1536.

[8] A.M. Hassan, A.A. Alwan, & H.K. Hamzah, "Metallic foam with cross flow heat exchanger: A review of parameters, performance, and challenges," *Heat Transf.*, 2023, vol. 52, pp. 2618-2650.

[9] S. Wang, X. Hou, J. Yin, Y. Xing, & Z. Wang, "Comparative study of the thermal enhancement for spacecraft PCM thermal energy storage units", *Aerospace*, 2022, vol. 9, pp. 705.

[10] Q. Guan, Y.F. Yap, H. Li, & Z. Che, "Modeling of nanofluid-fluid two-phase flow and heat transfer", *Int. J. Comput. Methods*, 2018, vol. 15, pp. 1850072.

[11] A.D. Brent, V.R. Voller, & K.J. Reid, "Enthalpy-porosity technique for modeling convection-diffusion phase change: Application to the melting of a pure metal", *Num. Heat Transf.,* 1988, vol. 13 pp. 297-318.

[12] S. Kim, M.C. Kim, & B. Lee, "Numerical analysis of convection driven melting and solidification in a rectangular enclosure", *J. Ind. Eng. Chem.,* 2002, vol. 8, pp. 185-190.

[13] Y.A. Cengel, J.M. Cimbala, & R.H. Turner, "*Fundamentals of thermal-fluid science: SI units (3rd ed.)*", 2008, McGraw Hill Higher Education.

[14] W. Wang, L. Ding, F. Han, Y. Shuai, B. Li, B., & B. Sunden, "Parametric study on thermo-hydraulic performance of NACA airfoil fin PCHEs channels", *Energies*, 2022, vol. 15, pp. 5095.

[15] R.G. Allen, "Relating the Hazen-Williams and Darcy-Weisbach friction loss equations for pressurized irrigation", *Appl. Eng. Agric.*, 1996, vol. 12, 685-693.